Journal of Biological Physics **28:** 383–394, 2002.

Different Scenarios for Inter-Protein Electron Tunneling: The Effect of Water-Mediated Pathways

O. MIYASHITA, H.L. AXELROD and J.N. ONUCHIC
University of California, San Diego, 9500 Gilman Dr, La Jolla, California, U.S.A.

Abstract. Recent theoretical developments now allow for reliable calculation of tunneling matrix elements in unimolecular biological electron transfer reactions that have been tested experimentally. Most biological ET processes, however, are *bi*molecular, or involve large-scale protein domain motions. In this paper, initial advances in this direction by studying the inter-protein electron transfer between cytochrome c_2 and the photosynthetic reaction center. Utilizing an approach that integrates molecular dynamics and the Pathways method, we have observed that the ensemble dominant tunneling pathways in this reaction go though the tyrosine 162 or are water mediated.

Key words: biological tunneling, pathways, photosynthetic reaction center, water mediated pathways

1. Introduction

Oxidative phosphorylation, drug metabolism, DNA damage, photosynthesis, and much of enzymatic catalysis occur *via* electron-transport (ET) processes. The last decade has seen tremendous growth in the development of reliable molecular-level theories and models for *unimolecular* biological electron transfer (ET) reactions [1–4]. These theories now allow the computation of donor-acceptor interactions (tunneling matrix elements) *via* empirical (Pathways [5, 6] and protein packing density analysis [7]), semi-empirical electronic structure methods (extended-Hückel [8–13], neglect of differential overlap methods [14, 15]), and *ab initio* divide-and-conquer methods [16–18]. Many unimolecular ET rates in proteins can be computed reliably, structure-function relations are emerging, and many useful predictions concerning coupling pathway structure and function can now be made *a priori*. Many examples exist where theoretical analysis has led to specific testable predictions [19], has led to the design of key mutagenesis experiments, or has helped to explain otherwise puzzling experimental results [20–23].

Most biological ET processes, however, are bimolecular, or involve large-scale protein domain motion. The combined problem of protein geometric fluctuation *and* ET is poorly treated with conventional unimolecular approaches. In this paper, we start to move in this direction by exploring a well-known inter-protein ET reaction. The membrane-bound photosynthetic reaction center (PC) and the water-soluble cytochrome c_2 (cyt c_2) proteins in the photosynthetic bacterium *Rbodobac-*

ter sphaeroides are key components of the photosynthetic apparatus used to convert light energy into chemical energy in the form of ATP [24–26]. In *Rb. Sphaeroides*, reduced cyt c_2 (cyt c_2^{2+}) is the primary electron donor to the photo-oxidized primary donor, a specialized bacteriochlorophyll dimer $(BChl)_2$, on the RC. *In vivo* and *in vitro*, cyt c_2 and RC form a transient electron transfer complex. Electron transfer within the bound complex is rapid, occurring at a rate of 10^6 s^{-1} [27, 28]. This ET reaction has been extensively investigated by site-directed mutagenesis [29], computational-based docking [30, 31], chemical modification [32], and linear dichroism [33]. The goal of these investigations have been to further our understanding of the ET reaction between cyt c_2 and RC at the molecular level. A primary point of interest is the influence of the protein environment at the binding interface on the electron transfer rate.

Recently Axelrod *et al.* have obtained the X-ray structure on a co-crystal of the RC and cyt c_2 [34, 35, 57]. The three-dimensional structure shows that a tyrosine residue, TYR L162, on the L subunit of the RC, is located in a small pocket protruding from the periplasmic surface, and in van der Waals contact of both the heme on cyt c_2 and the $(BChl)_2$ on the RC. A homologous tyrosine residue is located in the structure of the RC from *Rhodopseudomonas viridis* in which a permanently-bound tetraheme cytochrome is the electron donor to the photo-oxidized $(BChl)_2$ [36, 37]. Several investigators have thus proposed that tyrosine L162 might play an important role, possibly by facilitating electron transfer between the cytochrome and RC. Do all the important tunneling pathways in this reaction have to go through this tyrosine? By integrating molecular dynamics techniques with the Pathways methods, we can now start to answer this question.

2. Methods

2.1. MOLECULAR DYNAMICS SIMULATION

We have carried out a molecular dynamics simulation of the cyt c_2: RC from *Rhodobacter sphaeroides*. For the simulations, refined coordinates of the cyt c_2: RC complex without modeled water molecules were obtained from X-ray studies by Axelrod *et al.* [34, 35, 57]. Additional water molecules were placed to fill a sphere of 30 Å radius centered on the iron of the heme. Since the X-ray structure of the complex shows that cyt c_2 interacts with only the L and M subunits, the H unit of RC was excluded in order to reduce the size of the system to be simulated. Figure 1 shows the structure of the complex prior to simulations. The total number of explicit water molecules included in this system is 1730. We used partial charges published previously for the reduced heme group [38]. For the oxidized heme group, we used the charge reported in a previous study on cytochrome *c* [39, 40], which was prepared by using a charge distribution of reduced and oxidized porphines [41]. The partial charges of the reduced and oxidized bacteriochlorophyll, bacteriopheophytin, and ubiquinone RC cofactors were prepared by restricted and unrestricted Hartree Fock calculations with the PM3 basis set using the GAMESS

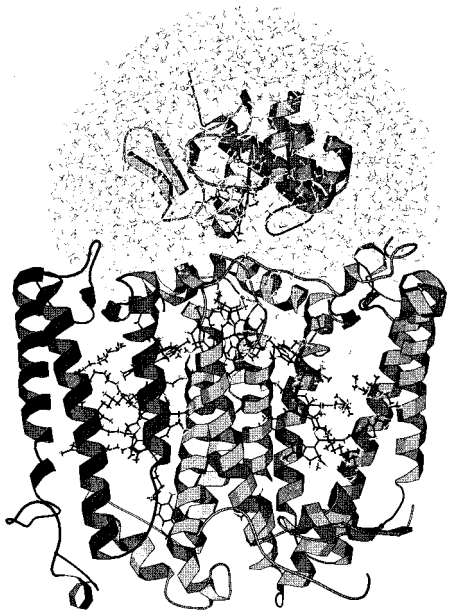

Figure 1. A schematic representation of the prepared structure for the 'solvated' complex of cytochrome c_2 and the photosynthetic reaction center utilized in our calculations. H unit is not included in the simulation.

package [42]. Additional parameters for these compounds are taken from standard AMBER parameter set [43]. The AMBER94 force field [43] was used for the protein atoms, and the TIP3P model was used for water molecules [44].

We used AMBER6 program package [45] to carry out the molecular dynamics simulation. A dielectric constant of $\varepsilon = 4$ was used. A CAP boundary potential was used to constrain the position of watermolecules near the protein. Long-range interactions were treated with a 20 Å cutoff. Weak constraints were imposed on the main chain atoms to keep the shape of RC and to prevent dissociation of the cyt c_2 from the RC. The energetic contribution from the constraints is less than 1% of the total energy; thus it is enough weak to provide some flexibility to the main chain. The positions of the sidechain atoms were not constrained. Energy minimization was performed for the initial X-ray coordinates with a suitable combination of the steepest descent and the conjugate gradient techniques. Following the energy minimization, a 100psec molecular dynamics simulation was carried out to equilibrate the system at 300 K. Finally a one nsec simulation run was used to generate the ensemble of structures used in this study. The coordinates for structures in this trajectory were stored at every one psec. The minimization and the molecular dynamics simulation were performed with the heme on cyt c_2 in the reduced state (cyt c_2^{2+}) and the $(BChl)_2$ on the RC in the photo-oxidized radical cation state $(BChl)_2^+$. Thus, the reaction investigated is cyt c_2^{2+}: $RC^+ \rightarrow$ cyt c_2^{3+}: RC.

2.2. THE PATHWAYS MODEL AND TUNNELING MATRIX ELEMENT CALCULATIONS

In long distance electron transfer reactions, the electronic coupling between donor and acceptor is sufficiently weak that most reaction occur in the non-adiabatic regime. The rate for non-adiabatic electron transfer can be written utilizing Fermi's Golden Rule [3, 46, 47] by,

$$k_{\mathrm{ET}} = \frac{2\pi}{\hbar}|T_{\mathrm{DA}}|^2 \ (\mathrm{F.C.}) \tag{1}$$

where (F.C.) is the Franck-Condon factor associated with the nuclear motion along the reaction coordinate, and T_{DA} is the electronic tunneling matrix element for the electron donor (D)-acceptor (A) pair.

The tunneling pathways model assumes that a few pathways or tubes control this electronic coupling between donor and acceptor, and as such seeks these dominant paths. The numerical implementation of this method assigns a 'decay' factor for the different kind of contacts in a protein. An electron tunneling pathway is defined as a product of these decays via covalent (C), hydrogen bonded (H), or through-space (S) connections. For a single pathway, the coupling is approximated as [48–50]

$$T_{\mathrm{DA}} \propto \prod_i \varepsilon_i^C \prod_j \varepsilon_j^S \prod_k \varepsilon_k^H . \tag{2}$$

As a simple implementation of the pathway model, we chose the following parameters [5, 51].

$$\varepsilon^C = 0.6 \tag{3}$$

$$\varepsilon^H = (0.6)^2 \exp[-1.7(R - 2.8)] \tag{4}$$

$$\varepsilon^S = 0.6 \exp[-1.7(R - 1.4)]. \tag{5}$$

The distances between heavy atoms, R, are in angstroms and the decay factors, ε, are unitless. These relationships have been used to predict the electronic coupling decay along specific pathways in some electron transfer proteins such as azurin and cytochrome c [5, 51].

For each transient structure stored during molecular dynamics simulation, we carried out calculations to determine the specific pathway that maximizes the heme-$(\mathrm{BChl})_2$ electronic coupling. A program incorporating the algorithm of Betts *et al.* [52] was coded in JAVA language and used for our pathway calculations. In these pathway calculations, water molecules included in the molecular dynamics were considered to be functional components for electron tunneling.

For our pathway calculations hydrogen-bond couplings are distance-scaled as in a standard model [5, 51]. An alternative model [20, 53] that treats the hydrogen

bonds as covalent bonds, i.e., $\varepsilon_H = \varepsilon_c^2$, but we have not used it here since the hydrogen bonds at the interface between the proteins are likely to exhibit a larger range of distances than hydrogen bonds in the core of the protein. In this interface, hydrogen bonds are made and broken between water molecules and the protein surfaces and therefore much less constrained than inside the protein. These hydrogen bonds versus those between protein atoms, whose positions are more constrained.

3. Results and Discussion

Although there are several pathways with sufficiently large coupling to influence electron tunneling in this interface, in this paper we restrict ourselves to show the results only for the most dominant path for each sampled structure. This dominant path is sufficient to identify the best tube between the donor and acceptor and to provide a reasonable quantification of this coupling. As it becomes apparent in the results that follow, this dominant tube fluctuates between the ones that go through a direct contact between the two proteins via the tyrosine L162 and the ones that are mediated by water. This result strongly supports that structural fluctuations cannot be ignored when investigating inter-protein ET and that the dominant tube obtained for the static crystal structure provides an incomplete description of the tunneling mechanism.

3.1. THE DOMINANT PATHWAY IN THE X-RAY STRUCTURE

The primary goal of our investigation is to determine how conformational fluctuation of protein atoms in the complex affects the tunneling matrix elements. Before we do that, as a reference for comparison, we calculate the Pathways decay for the crystal structure of the cyt c_2:RC complex. The calculations show a maximum pathways decay of approximately 6×10^{-5} along a pathway of atoms from the heme to a ring on the RC donor, $(BChl)_2$ that includes HEME:CBC $\rightarrow$ L162TYR:CE1 $\rightarrow$ L162TYR:CZ $\rightarrow$ L162TYR:CE2 $\rightarrow$ $(BChl)_2$:CBC. There are two through space jumps along this pathway; 1) 3.3 Å jump from HEME:CBC to L162TYR:CE1 and 2) a 4.0 Å through-space jump from L162TYR:CE2 to the special pair group DA:CBC. Gray and collaborators [20] have proposed that the rate for electron transfer in proteins, when they have their Franck-Condon factor optimized, can be written as $k_{ET} \sim 10^{14}$ *or* 10^{13} $s^{-1} \times$ (Pathways decay)^2. If we choose the larger prefactor, this decay would provide an ET rate of approximately 0.4×10^6 s^{-1}, which is in reasonable agreement with the experimentally observed rate of 10^6 s^{-1}.

3.2. STRUCTURAL VARIATION OF THE TUNNELING MATRIX ELEMENT

Figure 2 shows the variation in the electronic coupling, T_{DA}, observed during the one nsec trajectory of the molecular dynamics simulation. During this one nsec

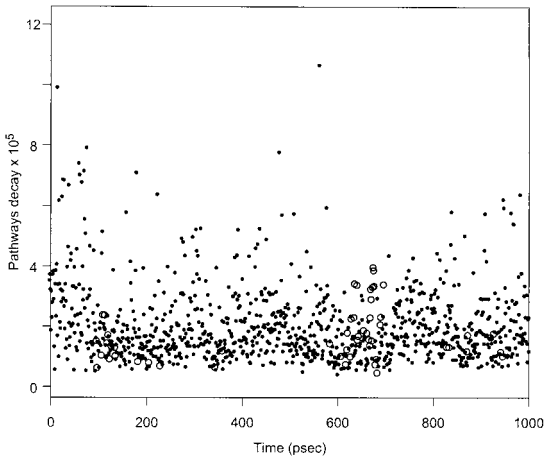

Figure 2. The values for the dominant Pathways decays for structure sampled during 1 nsec molecular dynamics run. Structures were recorded every 1 psec. For those structures that have a dominant pathway that include one water molecule, open circles instead of dots were used to plot their decays.

course of the simulations, 1000 structures were sampled at one psec intervals, and the dominant pathway of each structure was determined. Each point in this figure represents to the Pathways decay of the dominant parthway of each structure. A circle denotes those 54 structures whose pathways include water molecules.

Figure 3 shows how the magnitude of the Pathways decay is distributed over each of the 1000 structures. The average value of this decay is, over the time course of the simulation, 2.083×10^{-5}. We have calculated a decay of 5.70×10^{-5} for the X-ray structure, which is 2.7 times larger than average value from the simulation. We should note that those structures that include water molecules in their ET pathway show similar decays to the typical ones that go directly between the two proteins.

3.3. STRUCTURES WITH TYPICAL PATHWAYS

Figure 4(a) shows the most dominant pathway observed during the one nsec run. This pathway is superimposed on the X-ray structure to facilitate visualization. Most of the dominant pathways for the different structures go through L162TYR, which is suggested as the bridge for ET between the cyt c_2 and the RC [54]. The through space jump between the L162TYR:CD1 and the HEME:CBC group appears in most of these pathways, i.e., it can be found in the dominant path of 681 structures of the 1000 that we have sampled. Thus, the through space distance between these two atoms is an important factor in determining the strength of T_{DA}. The HEME:CBC also has an important role. 936 dominant pathways include a through space jump between the HEME:CBC group and one of the atoms in

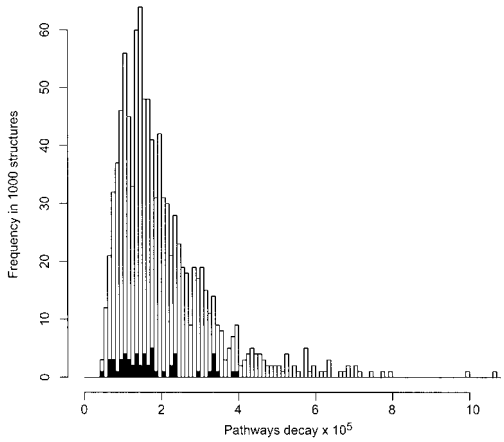

Figure 3. Distribution the Pathways decays for the 1000 sample structures. Width of the bins is 1×10^{-6}. Black colored regions of histogram indicate the occurrence dominant pathways that include water molecules. The three largest Pathway decays are 1.07×10^{-4}, 9.90×10^{-5}, and 7.91×10^{-5}. The three smallest ones are 4.07×10^{-6}, 4.62×10^{-6}, and 4.94×10^{-6}. The largest decays for dominant pathways that include one water molecule are 3.96×10^{-5}, 3.86×10^{-5}, and 3.42×10^{-5}. The three smallest ones are 4.62×10^{-6}, 6.26×10^{-6}, and 6.42×10^{-6}.

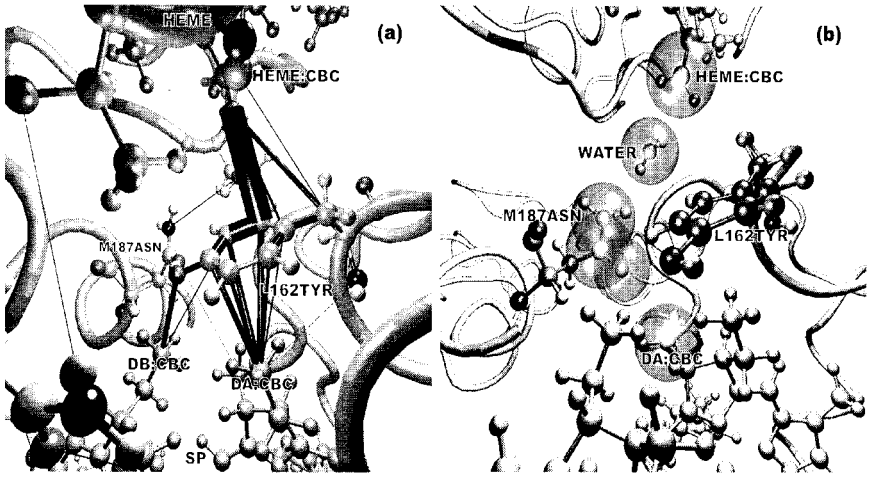

Figure 4. (a) Dominant pathways sampled during the one nsec run superimposed on the X-ray structure. Black lines connecting atoms represent covalent bonds; through space jumps; or hydrogen bonds involved the pathway. Thickness of the black lines is proportional to the frequency that each connection is included in the dominant pathways. Pathway connections that occur less than 10 times in the 1000 structures sampled are omitted. (b) A typical dominant pathway that includes one water molecule. Atoms included in the pathway are represented as large spheres. L162TYR is shown but it is not part of this dominant pathway.

L162TYR. Regarding the special pair, 733 dominant pathways are connected to the group CBC of DA, and of 127 ones are connected to the group CBC of DB.

Of the 1000 structures that have been sampled, the largest observed value for the Pathways decay is 1.07×10^{-4}. Atoms included in this pathway are HEME:CBC → L162TYR:CD1 → TYR:CG → TYR:CD2 → DA:CBC. The main reason for this large coupling is a small conformational rearrangement during thermal fluctuations that squeezes the through space jumps. No special contact of atoms is needed to make the matrix element especially large. The distance between the HEME:CBC group and the TYR162:CD1 is 3.58 Å and the distance between the TYR162:CD2 and the group DA:CBC is 3.39 Å, which are smaller than the typical ones.

The dominant pathway for 54 of these structures includes one water molecule. Each pathway includes at most one water molecule. These pathways include hydrogen bonds from/to water oxygen. The largest Pathways decay observed for these structures is 3.96×10^{-5}. A typical pathway with one water molecule, which has a decay of 2.90×10^{-5}, is shown in Figure 4(b): HEME:CBC → O of a water → M187ASN:ND2 → M187ASN:CG → M187ASN:ODI → DA:CMC. The interaction between the water and the ASN is a hydrogen bond. Most of these pathways go through M187ASN.

To better understand the effect of the water molecule in these pathways, we computed the strongest Pathway decay that does not include water for the structure above. A decay of 1.12×10^{-5}, about one third of the dominant one, was observed. In this structure, the through space jumps to/from TYR are longer than usual, e.g., the distance between the TYR162:CD1 and the HEME:CBC of this structure is of 5.5 Å. The atoms in this pathway contain main chain atoms, i.e., HEME:CBC → L162TYR:O → L162TYR:C → L162TYR:CA → L162TYR:N → DA:CBC. In addition, the through space jump between the HEME:CBC and the L162TYR:O is 3.80 Å and the one between the L162TYR:N and the DA:CBC is of 4.20 Å. Because of this minor structural disorder, the dominant tunneling tube now prefers to go through a water instead of L162Tyr.

4. Conclusion

The atoms included in the dominant pathway for the X-ray structure are common participants in most of the dominant pathways observed during one nsec run. This result indicates that tunneling matrix elements obtained from calculations utilizing the crystal structure can provide qualitative information about the tunneling pathway, but conformational fluctuations have to be incorporated for a more quantitative analysis. During our sampling run, the Pathways decay fluctuates about ten fold, i.e., one hundred fold in the rate. Most of these fluctuations are a consequence of the conformational rearrangement of L162TYR. The average decay from the distribution given in Figure 3 is about three times smaller than the decay from X-ray structure. This indicates that this crystal structure is better packed than the most of the ones observed in our simulation. Still, thermal fluctuations can lead

to decays even smaller than the X-ray one. Water molecules are included in the dominant pathways occasionally, i.e., in about 5% of the sampled structures. Still, dominant pathways with and without water have very similar coupling (same order of magnitude) and minor structural modifications makes one or the other slightly stronger. Tunneling therefore is dominated by this interplay between pathways that directly connect the two proteins and the water-mediated ones.

For the reasons described above, we expect that mutations on the surface of the protein would have a small effect on the tunneling matrix element as long as the overall complex structure is not changed. Water will move into any void at this interface, if needed, providing alternative pathways. This observation is consistent with the experimental results by Ortega *et al.* [54]. They studied electron transfer between the tetraheme cytochrome *c* and the special pair of bacteriochlorophylls in the reaction centers isolated from seven strains of the photosynthetic purple bacterium *Blastochloris viridis*. Mutations of the residue L162, located between the proximal heme $c-559$ and the special pair (Y (wild type) by F, W, G, M, T, or L) show almost no effect on the ET rate. For example, the rate for the mutation Y(L162) $\rightarrow$ G is only 5% slower than the wild type. Similar analysis for *Rb. Sphaeroids* would not be that direct since surface mutations may affect complex formation and stability [58].

Acknowledgements

Work in San Diego has been supported by the NIH (GM48043). O.M. acknowledges a research fellowship for young scientists from the JSPS, Japan. HLA also acknowledges Prof. George Feher for his NIH support (GM-13191). Computations have been done at the UCSD Keck II computing facility (partially supported by NSF-9970199) and the San Diego Supercomputer Center. Figure 1 was made with Molscript [55], and Figures 4 and 5 were made from VMD [56].

References

1. Bendall, D.S.: *Protein Electron Transfer*, BIOS Scientific Publishers, Oxford, 1996.
2. Cramer, W.A. and Knaff, D.B.: *Energy transduction in biological membranes*, Springer-Verlag, New York, 1990.
3. Marcus, R.A. and Sutin, N.: Electron Transfers in Chemistry and Biology, *Biochim. Biophys. Acta* **811** (1985), 265–322.
4. Bixon, M. and Jortner, J. (eds.): Electron transfer: from isolated molecules to biomolecules, *Adv. Chem. Phys.* **106**, (1999).
5. Beratan, D.N., Betts, J.N. and Onuchic, J.N.: Protein Electron Transfer Rates Set by the Bridging Secondary and Tertiary Structure, *Science* **252** (1991), 1285–1288.
6. Onuchic, J.N., Beratan, D.N., Winkler, J.R. and Gray, H.B.: Pathway Analysis of Protein Electron Transfer Reactions, *Annu. Rev. Biophys. Biomolec. Struct.* **21** (1992), 349–377.
7. Page, C.C., Moser, C.C., Chen, X.X. and Dutton, P.L.: Natural engineering principles of electron tunnelling in biological oxidation-reduction, *Nature* **402** (1999), 47–52.

8. Gehlen, J.N., Daizadeh, I., Stuchebrukhov, A.A. and Marcus, R.A.: Tunneling matrix element in Ru-modified blue copper proteins: Pruning the protein in search of electron transfer pathways, *Inorg. Chim. Acta* **243** (1996), 271–282.
9. Larsson, S.: Electron Transfer in Chemical and Biological Systems – Orbital Rules for Non-Adiabatic Transfer, *J. Am. Chem. Soc.* **103** (1981), 4034–4040.
10. Siddarth, P. and Marcus, R.A.: Electron Transfer Reactions in Proteins – an Artificial Intelligence Approach to Electronic Coupling, *J. Phys. Chem.* **97** (1993), 2400–2405.
11. Balabin, I.A. and Onuchic, J.N.: A new framework for electron transfer calculations – Beyond the Pathways-like models, *J. Phys. Chem. B* **102** (1998), 7497–7505.
12. Okada, A., Kakitani, T. and Inoue, J.: Nonperturbative Calculation of Electronic Coupling for Electron Transfer Reaction in Proteins, *J. Phys. Chem.* **99** (1995), 2946–2948.
13. Kawatsu, T., Kakitani, T. and Yamato, T.: Worm model for electron tunneling in proteins: Consolidation of the pathway model and the Dutton plot, *J. Phys. Chem. B* **105** (2001), 4424–4435.
14. Broo, A. and Larsson, S.: Electron Transfer in Azurin and the Role of Aromatic Side Groups of the Protein, *J. Phys. Chem.* **95** (1991), 4925–4928.
15. Wolfgang, J., Risger, S.M., Priyadarshy, S. and Beratan, D.N.: Secondary structure conformations and long range electronic interactions in oligopeptides, *J. Phys. Chem. B* **101** (1997), 2986–2991.
16. Kurnikov, I.V. and Beratan, D.N.: Ab initio based effective Hamiltonians for long-range electron transfer: Hartree-Fock analysis, *J. Chem. Phys.* **105** (1996), 9561–9573.
17. Marchi, M., Gehlen, J.N., Chandler, D. and Newton, M.: Diabatic Surfaces and the Pathway for Primary Electron Transfer in a Photosynthetic Reaction Center, *J. Am. Chem. Soc.* **115** (1993), 4178–4190.
18. Wang, J. and Stuchebrukhov, A.A.: DFT calculation of electron tunneling currents: Real-space (grid) molecular orbitals vs. Gaussian-type molecular orbitals, *Int. J. Quantum Chem.* **80** (2000), 591–597.
19. Skourtis, S.S. and Beratan, D.N.: In: G.W. Canters and E. Vijgenboom (eds.), *Biological Electron Transfer Chains: Genetics, Composition, and Mode of Operation*, Kluwer Academic Publishers, The Netherlands, 1998, pp. 9–27.
20. Gray, H.B. and Winkler, J.R.: Electron transfer in proteins, *Annu. Rev. Biochem.* **65** (1996), 537–561.
21. Winkler, J.R., Di Bilio, A.J., Farrow, N.A., Richards, J.H. and Gray, H.B.: Electron tunneling in biological molecules, *Pure Appl. Chem.* **71** (1999), 1753–1764.
22. Derege, P.J.F., Williams, S.A. and Therien, M.J.: Direct Evaluation of Electronic Coupling Mediated by Hydrogen Bonds – Implications for Biological Electron Transfer, *Science* **269** (1995), 1409–1413.
23. Beratan, D.N., Onuchic, J.N., Winkler, J.R. and Gray, H.B.: Electron Tunneling Pathways in Proteins, *Science* **258** (1992), 1740–1741.
24. Graber, P. and Milazzo, G. (eds.): *Bioenergetics* **4**, Birkhauser Boston, MA, (1997).
25. Feher, G., Allen, J.P., Okamura, M.Y. and Rees, D.C.: Structure and Function of Bacterial Photosynthetic Reaction Centers, *Nature* **339** (1989), 111–116.
26. Tiede, D.M. and Dutton, P.L.: Electron transfer between reaction centers and mobile c-type-cytochromes, in: J. Deisenhofer and J.R. Norris (eds.), *The Reaction Center*, Academic Press, San Diego, CA, 1993, pp. 257–298.
27. Overfield, R.E., Wraight, C.A. and Devault, D.: Microsecond Photo-Oxidation Kinetics of Cytochrome-c_2 from *Rhodopseudomonas Sphaeroides* – Invivo and Solution Studies, *FEBS Lett.* **105** (1979), 137–142.
28. Rosen, D., Okamura, M.Y., Abresch, E.C., Valkirs, G.E. and Feher, G.: Interaction of Cytochrome-C with Reaction Centers of *Rhodopseudomonas Sphaeroides* R-26 – Localization

of the Binding-Site by Chemical Cross-Linking and Immunochemical Studies, *Biochemistry* **22** (1983), 335–341.
29. Tetreault, M., Rongey, S.H., Feher, G. and Okamura, M.Y.: Interaction between cytochrome *c*(2) and the photosynthetic reaction center from *Rhodobacter sphaeroides*: Effects of charge-modifying mutations on binding and electron transfer, *Biochemistry* **40** (2001), 8452–8462.
30. Adir, N., Axelrod, H.L., Beroza, P., Isaacson, R.A., Rongey, S.H., Okamura, M.Y. and Feher, G.: Co-crystallization and characterization of the photosynthetic reaction center-cytochrome *c*(2) complex from *Rhodobacter sphaeroides*, *Biochemistry* **35** (1996), 2535–2547.
31. Allen, J.P., Feher, G., Yeates, T.O., Komiya, H. and Rees, C.D.: Structure of the Reaction Center from *Rhodobacter Sphaeroides* R-26 – the Protein Subunits, *Proc. Natl. Acad. Sci. USA* **84** (1987), 6162–6166.
32. Long, J.E., Durham, B., Okamura, M. and Millett, F.: Role of Specific Lysine Residues in Binding Cytochrome-C2 to the *Rhodobacter Sphaeroides* Reaction Center in Optimal Orientation for Rapid Electron Transfer, *Biochemistry* **28** (1989), 6970–6974.
33. Drepper, F. and Mathis, P.: Structure and function of cytochrome *c*(2) in electron transfer complexes with the photosynthetic reaction center of *Rhodobacter sphaeroides*: Optical linear dichroism and EPR, *Biochemistry* **36** (1997), 1428–1440.
34. Axelrod, H.L., Abresch, E., Isaacson, R., Tetreault, M., Okamura, M.Y. and Feher, G.: Co-crystals of the RC cyt *c*(2) complex from *Rhodobacter sphaeroides*. With an improved cyt *c*(2) RC ratio, *Biophys. J.* **74** (1998), A146–A146.
35. Axelrod, H.L., Abresch, E.C., Okamura, M.Y., Feher, G., Yeh, A.P. and Rees, D.C.: X-ray structure determination of the RC-cyt *c*(2) complex from *Rhodobacter sphaeroides*, *Biophys. J.* **76** (1999), A20.
36. Deisenhofer, J., Epp, O., Miki, K., Huber, R. and Michel, H.: Structure of the Protein Subunits in the Photosynthetic Reaction Center of *Rhodopseudomonas Viridis* at 3a Resolution, *Nature* **318** (1985), 618–624.
37. Deisenhofer, J., Epp, O., Sinning, I. and Michel, H.: Crystallographic Refinement at 2.3-Angstrom Resolution and Refined Model of the Photosynthetic Reaction Center from *Rhodopseudomonas Viridis*, *J. Mol. Biol.* **246** (1995), 429–457,
38. Northrup, S.H., Pear, M.R., Morgan, J.D., McCammon, J.A. and Karplus, M.: Molecular Dynamics of Ferrocytochrome-C – Magnitude and Anisotropy of Atomic Displacements, *J. Mol. Biol.* **153** (1981), 1087–1109.
39. Miyashita, O. and Go, N.: Pressure dependence of protein electron transfer reactions: Theory and simulation, *J. Phys. Chem. B* **103** (1999), 562–571.
40. Miyashita, O. and Go, N.: Reorganization energy of protein electron transfer reaction: Study with structural and frequency signature, *J. Phys. Chem. B* **104** (2000), 7516–7521.
41. Kashiwagi, H. and Obara, S.: Abinitio Molecular Orbital Calculation of Fe-Porphine with a Double Zeta-Basis Set, *Int. J. Quantum Chem.* **20** (1981), 843–859.
42. Schmidt, M.W., Baldridge, K.K., Boatz, J.A., Elbert, S.T., Gordon, M.S., Jensen, J.H., Koseki, S., Matsunaga, N., Nguyen, K.A., Su, S.J., Windus, T.L., Dupuis, M. and Montgomery, J.A.: General Atomic and Molecular Electronic Structure System, *J. Comput. Chem.* **14** (1993), 1347–1363.
43. Cornell, W.D., Cieplak, P., Bayly, C.I., Gould, I.R., Merz, K.M., Ferguson, D.M., Spellmeyer, D.C., Fox, T., Caldwell, J.W. and Kollman, P.A.: A 2nd Generation Force-Field for the Simulation of Proteins, Nucleic Acids, and Organic Molecules, *J. Am. Chem. Soc.* **117** (1995), 5179–5197.
44. Jorgensen, W.L., Chandrasekhar, J., Madura, J.D., Impey, R.W. and Klein. M.L.: Comparison of Simple Potential Functions for Simulating Liquid Water, *J. Chem. Phys.* **79** (1983), 926–935.
45. Case, D.A., Pearlman, D.A., Caldwell, J.W., III, T.E.C., Ross, W.S., Simmerling, C.L., Darden, T.A., Merz, K.M., Stanton, R.V., Cheng, A.L., Vincent, J.J., Crowley, M., Tsui, V., Radmer,

R.J., Duan, Y., Pitera, J., Massova, I., Seibel, G.L., Singh, U.C., Weiner, P.K. and Koll-man, P.A.: *Amber 6*, University of California, San Francisco, 1999.
46. Hopfield, J.J.: Kinetic Proofreading: A New Mechanism for Reducing Errors in Biosynthetic Processes Requiring High Specificity, **71** (1974), 4135–4139.
47. Jortner, J.: Temperature-Dependent Activation-Energy for Electron-Transfer between Biological Molecules, *J. Chem. Phys.* **64** (1976), 4860–4867.
48. Beratan, D.N. and Onuchic, J.N.: Electron-Tunneling Pathways in Proteins – Influences on the Transfer Rate, *Photosynth. Res.* **22** (1989), 173–186.
49. Beratan, D.N., Onuchic, J.N. and Hopfield, J.J.: Electron Tunneling through Covalent and Noncovalent Pathways in Proteins, *J. Chem. Phys.* **86** (1987), 4488–4498.
50. Onuchic, J.N. and Beratan, D.N.: A Predictive Theoretical Model for Electron Tunneling Pathways in Proteins, *J. Chem. Phys.* **92** (1990), 722–733.
51. Beratan, D.N., Onuchic, J.N., Betts, J.N., Bowler, B.E. and Gray, H.B.: Electron Tunneling Pathways in Ruthenated Proteins, *J. Am. Chem. Soc.* **112** (1990), 7915–7921.
52. Betts, J.N., Beratan, D.N. and Onuchic, J.N.: Mapping Electron Tunneling Pathways – an Algorithm That Finds the Minimum Length Maximum Coupling Pathway between Electron Donors and Acceptors in Proteins, *J. Am. Chem. Soc.* **114** (1992), 4043–4046.
53. Regan, J.J., Dibilio, A.J., Langen, R., Skov, L.K., Winkler, J.R., Gray, H.B. and Onuchic, J.N.: Electron Tunneling in Azurin – the Coupling across a Beta-Sheet, *Chem. Biol.* **2** (1995), 489–496.
54. Ortega, J.M., Dohse, B., Oesterhelt, D. and Mathis, P.: Low-temperature electron transfer from cytochrome to the special pair in *Rhodopseudomonas viridis*: Role of the L162 residue, *Biophys. J.* **74** (1998), 1135–1148.
55. Kraulis, P.J.: Molscript – a Program to Produce Both Detailed and Schematic Plots of Protein Structures, *J. Appl. Crystallogr.* **24** (1991), 946–950.
56. Humphrey, W., Dalke, A. and Schulten, K.: VMD: Visual molecular dynamics, *J. Mol. Graph.* **14** (1996), 33–38.
57. Axelrod, H.L., Abresch, E.C., Okamura, M.Y., Yeh, A.P., Rees, D.C. and Feher, G.: X-ray structure determination of the cytochrome c_2:reaction center electron transfer complex from *Rhodobacter sphaeroides J. Mol. Biol.* (2002), in press.
58. Wachtveitl, J., Farchaus, J.W., Mathis, P. and Oesterhelt, D.: Tyrosine 162 of the photosynthetic reaction center L-subunit plays a critical role in the cytochrome c_2 mediated rereduction of the photooxidized bacteriochlorophyll dimer *Rhodobacter sphaeroides*. 2. Quantitative kinetic analysis. *Biochemistry*, **32** (1993), 10894–10604.